Multi-criteria Optimization for the Design and Operation of Distributed Energy Systems Considering Sustainability Dimensions

Juan Fonseca, Jean-Marc Commenge, Mauricio Camargo, Laurent Falk, Iván Gil

Energy 214 (2021) 118989

Contents lists available at ScienceDirect

Energy

journal homepage: www.elsevier.com/locate/energy

Multi-criteria optimization for the design and operation of distributed energy systems considering sustainability dimensions

Juan D. Fonseca [a, c, *], Jean-Marc Commenge [b], Mauricio Camargo [a], Laurent Falk [b], Iván D. Gil [c]

[a] Équipe de Recherche sur Les Processus Innovatifs (ERPI), Université de Lorraine, 8 Rue Bastien Lepage, 54000, Nancy Cedex, France
[b] Laboratoire Réactions et Génie des Procédés (LRGP), Université de Lorraine, 1 Rue Grandville, BP 20451, 54001, Nancy Cedex, France
[c] Grupo de Procesos Químicos y Bioquímicos, Department of Chemical and Environmental Engineering, Universidad Nacional de Colombia – Sede Bogotá, Carrera 30 45-03, Bogotá, Colombia

ARTICLE INFO

Article history:
Received 26 February 2020
Received in revised form
19 September 2020
Accepted 30 September 2020
Available online 8 October 2020

Keywords:
Renewable energy
Power-to-gas
Multi-energy system
Seasonal storage
Energy system design
Social criterion

ABSTRACT

The growing concerns about climate change and energy security have led to a shift in the paradigm of the energy framework. In this regard, distributed generation offers the possibility to deal with inefficiencies in energy delivering, and the fossil fuel dependence of conventional and centralized power plants. This work presents a modeling and multi-criteria optimization strategy for designing and operating decentralized power plants including different energy vectors. The modeling approach considers the time-varying operation of the energy conversion units for responding to electricity and hydrogen demands, along with the seasonal behavior of the storage system. A multi-criteria evaluation addressing economic, environmental and social aspects was implemented. The objective functions are the total annualized cost, the CO_2 emissions and the grid dependence. According to optimization results, it is highlighted the influence of the assessed criteria upon the structure and the operating policy of the power plant. Additionally, by comparing the performance of the distributed energy system with respect to a centralized scenario, it is noted the significant potential of the decentralized generation. Indeed, depending on the optimization goal, CO_2 emission reduction up to 89%, and self-sufficiency up to 81% can be achieved.

1. Introduction

Distributed or decentralized energy systems (DES) refer to small-scale generation units, i.e. typically with a capacity lower than 1000 kW, and located close to the end-consumers [1,2]. This kind of energy plants are focused on covering local demands, e.g. building, neighborhood, university campus or hospitals, by using specific on-site energy sources. In addition to a variety of resources, that can be renewable or conventional, DES include multiple conversion and storage technologies for supplying different demands (e.g. power, heating, cooling, fuel). Distributed generation offers a reliable, flexible and efficient alternative for the energy transition. DES also reduce the energy losses in transmission and delivery (characteristic of centralized plants), promote the use of renewable energies (which are location-dependent and not easily transported), favor the coupling between different energy forms, boost the energetic self-sufficiency and support the energy security [2–4].

Among the diversity of energy carriers that can be involved in DES, hydrogen has the potential to play a key role in energy transition. It is a versatile compound that can be obtained from a variety of sources such as fossil fuels, renewables, nuclear and biomass [5]. Additionally, hydrogen as storage medium can enhance the renewables deployment by providing a mid (weeks) or even long-term (months) alternative to trade-off the mismatch between electricity availability and demand [6,7]. In this application, hydrogen offers an option with reduced self-discharge rate, that could be reconverted into electricity when required, but also into methane (biomethane) through the power-to-gas pathway [8]. Broadly, hydrogen can contribute to a reliable, secure, resilient, and decarbonized energy system by enabling the sector coupling, and exploiting the synergies among different energy forms [2,6,7,9].

* Corresponding author. Équipe de Recherche sur les Processus Innovatifs (ERPI), Université de Lorraine, 8 rue Bastien Lepage, 54000, Nancy Cedex, France.
E-mail address: jdfonsecag@unal.edu.co (J.D. Fonseca).

https://doi.org/10.1016/j.energy.2020.118989

Nomenclature

PV_T	Total power generated by photovoltaics (kW)
EG_D	Grid power for electricity demand (kW)
I	Solar irradiance (kW/m^2)
PV_D	Photovoltaic power for electricity demand (kW)
I_{NOCT}	Solar irradiance at test conditions (kW/m^2)
PV_S	Surplus electricity from photovoltaics (kW)
T_a	Ambient temperature (°C)
EG_T	Total electricity imported from the grid (kW)
T_{ref}	Temperature at reference conditions (°C)
C	Capital cost (€/kW − €/kWh − €/m^2)
T_{NOCT}	Nominal operating cell temperature (°C)
k	Technology index
n_{pv}	Photovoltaics efficiency
Cap	Capacity of technology (kW − kWh − m^2)
n_s	Photovoltaics efficiency at reference conditions
r	Discount rate
A	Area of photovoltaics (m^2)
$O\&M_F$	Fixed operational and maintenance costs
El_{in}- El_{in}	Input-output electrolyzer power (kW)
OC_V	Variable operation costs
n_{El}	Electrolyzer efficiency
C_{EG}	Price of importing electricity (€/kWh)
$H_{2,El}$	Hydrogen produced by electrolysis (kW)
C_{NG}	Price of importing gas (€/kWh)
LHV_{H2}	Low heating value of hydrogen (kJ/kg)
C_{Bio}	Price of gathering biomass (€/ton)
PV_{H2}	Photovoltaic power used in the electrolyzer (kW)
AGE_p	Annual CO_2 emissions from process operations
EG_{H2}	Grid power used in the electrolyzer (kW)
AGE_G	Annual CO_2 emissions from importing energy
FC_{in}- FC_{out}	Input-output fuel cell power (kW)
AGE_B	Annual CO_2 emissions of processing biomass
n_{FC}	Efficiency of the fuel cell
BE_{AD}	Emissions from anaerobic digestion (kgCO_2/year)
S_B	Energy stored in the battery (kWh)
BE_{ref}	Emissions from biomethane reforming (kgCO_2/year)
B_{in}- B_{out}	Input-output power to the battery (kW)
IG	Energy imported from the grid (kWh)
n_{ch}	Charging efficiency of battery
TD	Total energy demanded by users (kWh)
n_{dch}	Discharging efficiency of battery
$H_{2,ref}^{b,m}$	Hydrogen from reforming of biomethane (kg)
S_{H2}	Energy stored in hydrogen form (kWh)
$H_{2,ref}^{f,m}$	Hydrogen from reforming of methane (kg)
$S_{H2,in}$- $S_{H2,out}$	Input-output power to the hydrogen storage (kW)
$D_{el,M}$	Demand of electricity not covered by photovoltaics (kW)
R_{in}- R_{out}	Input-output power to the reformer (kW)
$H_{2,el}^{G}$	Hydrogen produced from grid electricity (kW)
n_R	Efficiency of reforming
$H_{2,el}^{PV}$	Hydrogen produced from photovoltaic electricity (kW)
NG_R	Methane from the network for reforming (kW)
J	Performance criterion
LHV_{CH4}	Low heating value of methane (kJ/m^3)
u	Decision variables
AD_{in}	Input biomass to the anaerobic digester (kg/s)
t	Time
$CH_{4,AD}$	Methane produced by biomass digestion (m^3/s)
AD_{out}	Anaerobic digester output power (kW)
n_{AD}	Yield of anaerobic digestion (m^3/kg volatile solids)
D_{el}	Demand of electricity (kW)

Greek letter

β	Temperature coefficient
τ	Self-discharge factor
ϕ	Source of electricity for demand
θ	Source of hydrogen
α	Source of electricity for electrolysis
δ	Electricity storage option
γ	Source of methane for reforming
λ	Emission factor (kgCO_2/kWh or kgCO_2/kgH_2)
ω	Deforestation rate

Acronym

DES	Distributed energy systems
CAPEX	Capital expenditure
OPEX	Operational expenditure
PSA	Pressure swing adsorption
TAC	Total annualized cost
AGE	Annual CO_2 emissions
CRF	Capital recovery factor
GD	Grid dependency

Despite the potential benefits of the decentralized generation and the use of hydrogen as energy carrier, the design and operation of this kind of plants are a challenging task. Firstly, time dependence of some input data, such as energy demand and availability of resources, requires special attention for considering a temporal resolution according to the design objectives [10]. Besides, evaluating a diversity of energy sources and assessing multiple technologies for energy conversion and storage, contribute to the problem complexity [10,11]. Furthermore, due to the close interaction of DES with community, designing this type of systems implies the assessment of socio-political dimension in addition to the economic and environmental aspects [12,13]. Consequently, this multi-criteria evaluation typically introduces stakeholders with conflicting objectives, which represents additional difficulties during decision-making process [11].

1.1. Research background

1.1.1. Time horizon representation in DES design

A significant amount of research about design and operation of distributed energy systems has been done considering different simulation periods and time-steps. Mehleri et al. developed an economic optimization dividing the full year calendar into 18 different periods (6 periods by day for 3 seasons) for the selection of the system components to satisfy the heat and power demands of a small neighborhood [14]. Yang et al. included cooling demand in the design of a district-scale system, and considered three types of typical days by year (winter, summer, and mid-season days), each one divided into 12 periods [15]. In other works, Schütz et al. used twelve typical demand days with hourly time resolution [16], and Pan et al. considered three typical days of the year (winter, summer

and transition season) [17].

Although these approaches are very useful for reducing the complexity of the optimization problem, they are not able to represent the seasonal behavior of the system due to the discontinuity between the characteristic periods. To tackle this issue, some few works have simultaneously considered a yearly horizon and the seasonal cycle of energy storage. On the one hand, the whole year has been modeled by using hourly time steps for designing district heating and cooling systems [18,19], and urban energy systems under the energy hub concept [20]. On the other hand, different approaches have been used for considering the whole year but reducing the complexity of the system, e.g. decomposing the optimization problem (separating the design and the operation) [21], coupling typical design days [22], considering typical periods [23], or employing time steps of 4 h [24].

1.1.2. Multi-criteria assessment in DES design

As previously mentioned, the planning of DES requires the consideration of criteria beyond the economic one. In this sense, some studies have included multi-objective functions for designing and/or operating these systems. On the one hand, some works have focused on the design of DES according to economic and environmental/exergetic criteria by using different representative periods. For instance, Pelet et al. modeled the electrical needs with 12 representative days, and considered economic and ecological criteria for the design of the system [25]; Li et al. developed a mixed integer linear programming (MILP) model for the optimal design of DES considering the total annualized cost and the CO_2 emissions as objective functions [26]; and Di Somma et al. carried out the optimization including economic and exergetic assessments in the design of DES [27]. In another work, Fazlollahi et al. addressed the MILP optimization problem by using the integer cut constrain (ICC) algorithm combined with the epsilon constraint method, and a multi-objective evolutionary algorithm [28]. Other works have focused on optimizing the operation of the system either by formulating deterministic multi-objective linear programming (MOLP) problems [29,30], or through stochastic models for including uncertainties on energy demand and supply [31]. The latter used Monte Carlo method and roulette wheel mechanism for modeling the uncertainty of energy price, solar availability, and user energy demand.

On the other hand, some studies have also addressed multi-criteria optimization problems, but considering energy storage and the whole year as time horizon. In this respect, Dorotić et al. have implemented economic, environmental and exergetic criteria for designing district heating systems [18], and a multi-objective problem based on minimizing the total costs and the CO_2 emissions in the design of heating and cooling systems [19]. Unlike those papers, that addressed the multi-objective problem by using the weighted sum method, other works have employed MILP and the epsilon constraint method for the optimal design of DES. In this regard, Maroufmashat et al. have employed the energy hub approach, and have focused on the energy exchange between hubs [20], whereas Gabrielli et al. have emphasized on the seasonal energy storage within the system [22]. Conversely, Dufo-López et al. used evolutionary and genetic algorithms to solve a triple-objective optimization problem including cost, pollutant emissions and unmet load as objective functions [32]. Moreover, Eriksson and Gray, considered a semi-quantitative socio-political index that represents the expected public satisfaction of a particular energy system in addition to the economic and environmental objectives [33].

1.2. Motivation and contribution of this paper

This overview shows the great diversity of research regarding the design and operation of decentralized energy systems. On the one hand, the optimal design of DES is formulated as a MILP problem, where binary variables are used for specifying whether a technology is installed or not, and for representing their on/off status at each time step. In this regard, although there are a variety of approaches for addressing MILP problems such as branch-and-bound, cutting plane or decomposition methods, it is also recognized that the complexity of solving this type of problems is higher than that one of a model only based on continuous variables [34,35]. On the other hand, the analysis has been predominantly concentrated on economic and environmental criteria, thus neglecting the influence of the social dimension in DES design. Indeed, when included, social aspects are accounted after to solve the optimization problem, so that they are not a criterion during the system design [36]. However, further than being economically feasible and environmentally friendly, industrial activities must agree with social requirements, i.e. to improve the quality of life [37,38]. Additionally, energy is a key component of the human life since it drives many aspects of economic and social growth (e.g. jobs, food production, incomes). Consequently, energy could be considered as nearly the prime challenge and opportunity that the world faces towards sustainable development, which involves economic success, social acceptance, and environmental protection [39].

In general, social criteria are focused on measuring the impact on the quality of life, and the perception or the preferences regarding certain technologies. In this regard, access to energy has been identified as paramount due to its implications on poverty, education, health and welfare issues [37,40]. In fact, lack of access to modern energy implies that people depend on inefficient and pollutant technologies for cooking and electricity services (mainly based upon traditional biomass, kerosene, and diesel) [39]. In addition to that, depletion and uncertain prices of fossil energy sources, risks derived from extreme weather conditions due to climate change, and possible political conflicts could affect the energy security even for people already connected to the grid [12,41]. Taking this into account, it is essential to design energy systems that promote the diversification of energy sources, the use of low-carbon technologies, and the reduction of imported energy for securing the energy provision [41–45]. In this respect, the energy import dependency has been recognized as a suitable indicator for assessing energy security since it is able to account for both, the amount of imported energy potentially avoided and the degree of self-sufficiency for providing access to energy [41,43,45,46].

Considering the foregoing aspects, the contribution of this work is twofold: first, an optimization approach for designing and operating DES only employing continuous variables is proposed; and secondly, economic, environmental and social criteria are assessed as objective functions for defining the optimal design and operation of the energy system. Thus, the remainder of the document is divided as follows. Initially, a general system flowsheet is described, and main energy sources, conversion units and energy demands are identified. Then, a mathematical model of the system and the optimization approach are presented. Afterwards, a case study is implemented to illustrate the proposed framework. Finally, three optimization problems are formulated and solved for the design and operation of the energy system. The optimization focused on minimizing the total annualized costs, the CO_2

emissions, and the grid dependence.

2. Methods

2.1. Energy system description

The considered energy system aims to satisfy electricity and hydrogen energy demand by using solar radiation, biomass, and the electricity and natural gas networks as energy inputs. The general flowsheet of the DES considered in this study is depicted in Fig. 1. Electricity demand is supplied through the photovoltaic panels and the electricity grid. During periods of high electricity production from photovoltaics, the surplus power can be stored in an electrical battery or in hydrogen form by using an electrolyzer and a pressurized tank. In the latter storing option, hydrogen might be reconverted into electricity when required by employing a fuel cell. Regarding hydrogen, it can be obtained by water electrolysis or methane reforming processes. In the former, the process is powered by both solar or grid-derived electricity, and the latter employs methane obtained from anaerobic digestion or the natural gas network.

2.2. System modeling

The proposed energy system model was built based upon two main considerations: (i) energy transformers with constant efficiency, and (ii) there is no energy losses across the connection lines.

- Photovoltaics: The power obtained from solar panels along time is presented in Equation (1). Additionally, Equation (2) describes the dependence of conversion efficiency upon the solar radiation and ambient temperature [47].

$$PV_T(t) = n_{PV}(t) I(t) A \tag{1}$$

$$n_{PV}(t) = n_s \left(1 - \beta \left[T_a(t) - T_{ref} + \left(T_{NOCT} - T_a(t)\right) \frac{I(t)}{I_{NOCT}}\right]\right) \tag{2}$$

Here, PV_T is the electrical power generated, n_{PV} the panel efficiency, I the solar radiation, and A represents the installed area. n_s is the panel efficiency at reference conditions, β the characteristic temperature coefficient, T_a the ambient temperature, T_{ref} the temperature at reference conditions, T_{NOCT} the nominal operating cell temperature, and I_{NOCT} its corresponding irradiance.

- Electrolyzer: In this unit, electricity is used to split water into hydrogen and oxygen. This energy conversion is expressed in terms of input-output power as presented in Equation (3). In that equation, El_{in} is the input electrical power, El_{out} the hydrogen produced, and n_{El} the efficiency of electrolysis.

$$El_{out}(t) = El_{in}(t) n_{El} \tag{3}$$

It is worth to note that according to the proposed energy system scheme (Fig. 1), the power supplied to the electrolyzer could come from both, the photovoltaic panels (PV_{H2}) and/or the electricity grid (EG_{H2}). Hence, the total input power (El_{in})

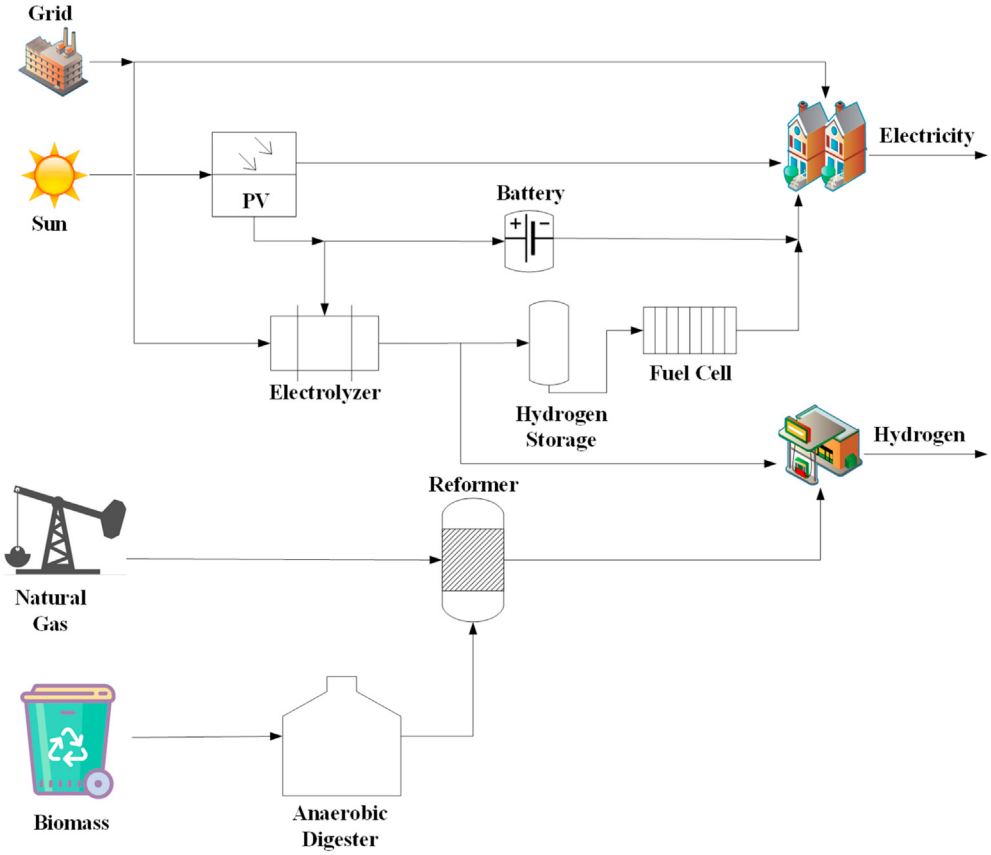

Fig. 1. Scheme of the studied energy system.

considers the contribution of these two sources as stated in Equation (4).

$$El_{in}(t) = PV_{H2}(t) + EG_{H2}(t) \quad (4)$$

- Fuel cell: In this equipment the reverse process of the electrolyzer is carried out, i.e. hydrogen and oxygen are fed for producing electricity and water. In this work, fuel cell is employed for obtaining electricity from hydrogen, if available in the storage system, and if there is not enough production from photovoltaics. As for the electrolyzer, the performance of the fuel cell is described by a characteristic efficiency (Equation (5)), where FC_{in} is the input power, FC_{out} the electricity produced, and n_{FC} the efficiency of the fuel cell.

$$FC_{out}(t) = FC_{in}(t)n_{FC} \quad (5)$$

- Energy storage: In this study, electrical battery and pressurized hydrogen tank are the storing energy alternatives. In both systems, the cycle energy losses are considered. For the battery, these losses depend on the charging/discharging efficiencies and the self-discharge, which is characteristic of these devices. Meanwhile, in the hydrogen system, the energy loss is due to the conversion efficiencies of the electrolyzer and fuel cell.

  Taking this into account, Equations (6) and (7) present the time-dependent balance for the battery and hydrogen storage systems, respectively.

$$S_B(t) = (1-\tau)S_B(t-\Delta t) + \left(B_{in}(t)n_{ch} - \frac{B_{out}(t)}{n_{dch}}\right)\Delta t \quad (6)$$

$$S_{H2}(t) = S_{H2}(t-\Delta t) + \left(S_{H2,in}(t) - S_{H2,out}(t)\right)\Delta t \quad (7)$$

  Here, S_B and S_{H2} represent the amount of energy stored at each time t in the battery and hydrogen system, respectively. τ is the self-discharging parameter of battery; n_{ch} and n_{dch} the corresponding charging and discharging efficiencies; B_{in} and B_{out} the input and output power to the battery; and $S_{H2,in}$ and $S_{H2,out}$ the corresponding input and output energy flowrates to the hydrogen storage tank.
- Reforming reactor: Steam reforming of methane is the dominant worldwide process for producing hydrogen. Broadly, it consists of three main steps: firstly, the catalytic reaction of methane with steam to produce syngas (Equation (8)); then, the water-gas-shift reaction (Equation (9)); and finally, the pressure swing adsorption (PSA) to purify the hydrogen.

$$CH_4 + H_2O \leftrightarrow 3H_2 + CO \quad (8)$$

$$CO + H_2O \leftrightarrow H_2 + CO_2 \quad (9)$$

  In this work, the unit called *reformer* in Fig. 1 represents the whole process, and it is used for obtaining hydrogen from methane taken from the gas network (NG_R) or from anaerobic digestion (AD_{out}). The performance is described by a global efficiency, which relates the methane supplied with the hydrogen produced as expressed in Equation (10). In that equation, n_R is the efficiency of reforming process, and R_{in} and R_{out} the input of methane and output of hydrogen in terms of power, respectively.

$$R_{out}(t) = R_{in}(t)n_R \quad (10)$$

  Equation (11) represents the contribution of the two sources of methane for reforming process. Where AD_{out} corresponds to the biomethane and NG_R to the methane from the network.

$$R_{in}(t) = AD_{out}(t) + NG_R(t) \quad (11)$$

- Anaerobic digester: In this biochemical process, biogas (mixture of CH_4 and CO_2) is obtained as the result of the action (in absence of oxygen) of microorganisms over the organic compounds of biomass. In addition to biogas, a solid residue (so-called digestate) results from the process, which after a treatment can be used as bio-fertilizer. Typically, methane represents around 70% (v/v) of the biogas, hence it needs to be upgraded to remove the undesired impurities (mainly CO_2). At commercial level, there is a wide range of options for biogas clean-up, with physical, chemical and pressure-based operations offering gas losses below 2%. Among them, the most widespread technologies are PSA, water or amine scrubbing, and membrane or cryogenic separations [48,49].

  Thus, the upgraded biomethane flow rate ($CH_{4,AD}$) as a function of time can be described by means of Equation (12). Meanwhile, the corresponding output power of anaerobic digestion process (AD_{out}) is presented in Equation (13).

$$CH_{4,AD}(t) = AD_{in}(t)n_{AD}n_{up} \quad (12)$$

$$AD_{out}(t) = CH_{4,AD}(t)LHV_{CH4} \quad (13)$$

  Here, AD_{in} represents the input biomass; n_{AD} is the yield to methane of the digestion process; n_{up} the recovery fraction of upgrading operation; and LHV_{CH4} the low heating value of methane.
- Overall energy balance: As aforementioned, the objective of the proposed energy system is to satisfy the time-dependent demands of electricity and hydrogen. Taking this into account, and considering the system configuration depicted in Fig. 1, the energy balance over each energy demand at each time step t is expressed in Equations (14) and (15).

$$D_{el}(t) = PV_D(t) + FC_{out}(t) + B_{out}(t) + EG_D(t) \quad (14)$$

$$D_{H2}(t) = H_{2,el}(t) + R_{out}(t) \quad (15)$$

Here, D_{el} and D_{H2} represent the demand of electricity and hydrogen, respectively, and EG_D is the power taken from the electricity grid. Meanwhile, $H_{2,el}$ and R_{out} are the hydrogen provided by electrolysis and reforming process, respectively. Additionally, the total power of electricity and natural gas imported from the grid at each time step are presented in Equations (16) and (17). In these equations, EG_{H2} represents the electricity imported from the grid for producing hydrogen by means of water electrolysis, and NG_R the natural gas taken form the network for steam reforming process.

$$EG_T(t) = EG_D(t) + EG_{H2}(t) \quad (16)$$

$$NG(t) = NG_R(t) \quad (17)$$

2.3. Optimization approach

The aim of this work is to find the best energy system configuration and operating regime according to economic, environmental and social criteria. These optimization objectives correspond to the total annualized cost (*TAC*), the annual CO_2 emissions (*AGE*), and the grid dependence (*GD*). Then, the next sections present the objective functions, decision variables and the formulation of the optimization problem.

2.3.1. Objective functions

Total annualized cost involves the investment and operational expenditures *CAPEX* and *OPEX*, respectively, as described in Equation (18).

$$TAC = CAPEX + OPEX \tag{18}$$

$$CAPEX = \sum_{k}^{K} C_k Cap_k CRF_k \tag{19}$$

$$CRF_k = \frac{r(1+r)^{Lk}}{(1+r)^{Lk}-1} \tag{20}$$

$$OPEX = O\&M_F + OC_V \tag{21}$$

$$O\&M_F = \sum_{k}^{K} O\&M_k \quad ; \quad O\&M_k = f(C_k) \tag{22}$$

$$OC_V = C_{EG}\int_{t0}^{tf} EG_T dt + C_{NG}\int_{t0}^{tf} NG dt + C_{Bio}\int_{t0}^{tf} AD_{in} dt \tag{23}$$

As stated in Equation (19), *CAPEX* depends upon the capital cost (C_k), the capacity (Cap_k), and the annuity factor (CRF_k) of each technology *k*. Besides, *r* represents the discount rate (7%) and L_k the lifetime of the equipment. Meanwhile, *OPEX* comprises the fixed operational and maintenance costs ($O\&M_F$) and the variable operation costs (OC_V), as expressed in Equation (21). In this study, $O\&M_k$ are considered as a percentage of the annual investment cost of the corresponding energy conversion and storage alternative (Equation (22)). Moreover, variable operational costs rely upon the amount of electricity and natural gas imported from the grid during the evaluated period t_f, and their corresponding prices C_{EG} and C_{NG} (Equation (23)). Also, variable costs include the cost of gathering the biomass for anaerobic digestion (C_{Bio}).

Annual CO_2 emissions (*AGE*) are expressed in Equation (24) as a function of three contributions: the process operations that release CO_2 (AGE_P), the electricity and natural gas imported from the grid (AGE_G), and the processing of biomass (AGE_B). As stated in Equation (25), process emissions correspond to those produced from reforming reaction by using methane from the network, i.e. only fossil-derived CO_2 emissions are considered. In that equation, λ_{ref} represents the emission factor of reforming process, and $H_{2,ref}^{f,m}$ is the total amount of hydrogen produced (in mass) by means of steam methane reforming of natural gas (Equation (26)).

Meanwhile, CO_2 emissions due to the imports of energy from the grid are described in Equation (27). This value depends upon the total amount of electricity and natural gas taken from the grid and their corresponding emission factors λ_{EG} and λ_{NG}, respectively.

$$AGE = AGE_P + AGE_G + AGE_B \tag{24}$$

$$AGE_P = \lambda_{ref} H_{2,ref}^{f,m} \tag{25}$$

$$H_{2,ref}^{f,m} = \frac{n_R}{LHV_{H2}}\int_{t0}^{tf} NG_R dt \tag{26}$$

$$AGE_G = \lambda_{EG}\int_{t0}^{tf} EG_T dt + \lambda_{NG}\int_{t0}^{tf} NG dt \tag{27}$$

Moreover, CO_2 derived from processes employing biomass correspond to biogenic emissions and are accounted as expressed in Equation (28). That expression includes the emissions from the anaerobic digestion of biomass (BE_{AD}), the subsequent reforming of biomethane (BE_{ref}), and the factor ω, that represents the deforestation rate. Indeed, taking into account the low deforestation in France, it can be assumed that the CO_2 emitted by biomass processing is equivalent to that employed by biomass in the photosynthesis process, i.e. the deforestation rate (ω) is zero [50].

Equation (29) presents the emissions derived from anaerobic digestion process as a function of the emission factor λ_{AD}, and the total amount of biomethane produced. In Equation (30), $H_{2,ref}^{b,m}$ represents the hydrogen obtained via reforming of biomethane (in mass), which can be computed by means of Equation (31).

$$AGE_B = \omega\left(BE_{AD} + BE_{ref}\right) \tag{28}$$

$$BE_{AD} = \lambda_{AD}\int_{t0}^{tf} CH_{4,AD} dt \tag{29}$$

$$BE_{ref} = \lambda_{ref} H_{2,ref}^{b,m} \tag{30}$$

$$H_{2,ref}^{b,m} = \frac{n_R}{LHV_{H2}}\int_{t0}^{tf} AD_{out} dt \tag{31}$$

Regarding social criterion, the self-sufficiency or grid dependence was the selected indicator (Equations (32)–(34)). Thus, grid dependence *GD* is computed as the ratio between the total energy imported from the grid (*IG*) and the total energy demanded by users (*TD*). The former is accounted by adding the electricity and natural gas imported from the grid (Equation (33)). The latter is the sum of the electricity and hydrogen demands along the evaluated time horizon (Equation (34)).

$$GD = \frac{IG}{TD}100 \tag{32}$$

$$IG = \int_{t0}^{tf} EG_T dt + \int_{t0}^{tf} NG dt \tag{33}$$

$$TD = \int_{t0}^{tf} D_{el} dt + \int_{t0}^{tf} D_{H2} dt \tag{34}$$

2.3.2. Decision variables

Concerning decision variables, as mentioned in the introduction (Section 1), the design of energy systems has been mainly addressed in the literature by employing integer binary variables, which are used to select the energy conversion technologies and to describe their on/off status. Conversely, in this work the implemented optimization approach only uses continuous variables. This was performed by considering that, once the energy demands are specified, and for a set of given performance parameters (conversion efficiencies), all the power inputs can be formulated as a function of the desired power outputs. For instance, taking as reference the demand of hydrogen (Equation (15)), the both options for supplying it ($H_{2,el}$ and R_{out}) can be interpreted as a fraction of the total demand, as stated in Equations (35)–(37).

$$H_{2,el}(t) = \theta_1(t) D_{H2}(t) \tag{35}$$

$$R_{out}(t) = \theta_2(t) D_{H2}(t) \tag{36}$$

$$D_{H2}(t) = H_{2,el}(t) + R_{out}(t) = \sum_{i}^{I=2} \theta_i(t) D_{H2}(t) \tag{37}$$

where θ_1 and θ_2 represent the fraction of hydrogen coming from water electrolysis and steam methane reforming process, respectively. Meanwhile, I corresponds to the number of alternatives for supplying the hydrogen demand.

Similarly, this approach can be extended for the remainder of decisions required across the energy system, i.e. the source for supplying the electricity demand, the electricity storage alternative, the source of methane for reforming process, and the source of electricity for water electrolysis, as described in Equations (38)–(41). Regarding the electricity demand, as observed in Fig. 1, the power supplied by photovoltaics (when available) is directly sent to satisfy the whole or a fraction of electricity demand. Therefore, that energy flow (PV_D) is not a decision variable of the system. Taking this into account, the decision must be taken over the energy not covered by photovoltaics ($D_{el,M}$). In such a way, as presented in Equation (38), three alternatives are considered: the electricity grid (EG_D), the fuel cell (FC_{out}), and the battery (B_{out}).

$$D_{el,M}(t) = FC_{out}(t) + B_{out}(t) + EG_D(t) = \sum_{i}^{I=3} \phi_i(t) D_{el,M}(t) \tag{38}$$

$$PV_S(t) = PV_{H2}(t) + B_{in}(t) = \sum_{i}^{I=2} \delta_i(t) PV_S(t) \tag{39}$$

$$R_{in}(t) = AD_{out}(t) + NG_R(t) = \sum_{i}^{I=2} \gamma_i(t) R_{in}(t) \tag{40}$$

$$H_{2,el}(t) = H_{2,el}^{PV}(t) + H_{2,el}^{G}(t) = \sum_{i}^{I=2} \alpha_i(t) H_{2,el}(t) \tag{41}$$

Here, PV_S is the surplus electricity from photovoltaics. Moreover, ϕ represents the fraction of electricity supplied by each alternative, δ is the fraction of surplus electricity sent to each storage option, γ the fraction of methane coming from the natural gas network or the anaerobic digester, and α the fraction of hydrogen produced by using electricity from the grid ($H_{2,el}^{G}$) or photovoltaics ($H_{2,el}^{PV}$). Additionally, I represents the number of alternatives for each decision within the system. For clarity, Fig. 2 shows the energy flows on the flowsheet of the system.

Summarizing, the set of optimization variables comprises the fractions θ, ϕ, δ, γ and α. Thus, according to Equations (37)–(41), there are eleven decision variables by time step. However, by adding a consistency relationship for each decision (Equation (42)), the number of optimization variables is reduced to six by time step.

$$\sum_{i}^{I} S_i(t) = 1 \quad S \ni \{\phi, \theta, \alpha, \delta, \gamma\} \tag{42}$$

Moreover, it is worth to note that the search space of the optimization problem can be more easily limited by using these fractions instead of the energy flows as decision variables. Thus, considering the fractions θ, ϕ, δ, γ and α, the values of decision variables will always be constrained between 0 and 1. Conversely, if the energy flows are used as optimization variables, it will be more difficult to establish their upper limit since the size of the equipment and the energy flows within the system are unknown. Accordingly, the proposed framework enables to have a standard formulation that can be used independently of the energy system scale.

According to the formulation presented in Equations (37)–(41), optimization variables correspond to operating profiles, since they are associated to the energy flows within the system. Meanwhile, design variables (i.e. capacity of energy converters) are determined by picking the highest energy flow rate through the corresponding unit. In such a way, the capacity of fuel cell is equivalent to the highest value of its output flow rate (FC_{out}), the capacity of the reforming reactor is given by the maximum flow rate R_{out}, and so on. In the same line, if there is no flow rate through a technology along the whole evaluated period, it means that such equipment does not need to be installed within the system. Additionally, it is worth to note that Fig. 2 depicts two electrolyzers, one powered by photovoltaics, and another one by the electricity grid. Nevertheless, that is just for illustrating the electricity sources for obtaining hydrogen, and to show that hydrogen sent to the pressurized tank only comes from renewable electricity. In fact, in practice there is only one electrolyzer and its capacity is defined by the sum of energy flow rates PV_{H2} and EG_{H2}.

2.3.3. Optimization problem

Based upon the energy system model, the objective functions, and the decision variables previously defined, three independent optimization problems are formulated for minimizing the total annualized cost (J_1), the CO_2 emissions (J_2), and the grid dependence (J_3). The mathematical formulation of the optimization problems is presented in Equations (43)–(53).

$$Minimize \quad J_1(u, x, t) = TAC \tag{43}$$

$$J_2(u, x, t) = AGE \tag{44}$$

$$J_3(u, x, t) = GD \tag{45}$$

$$Subject\ to \quad h = f(u(t), x(t), p, t) \quad , \ system\ model \tag{46}$$

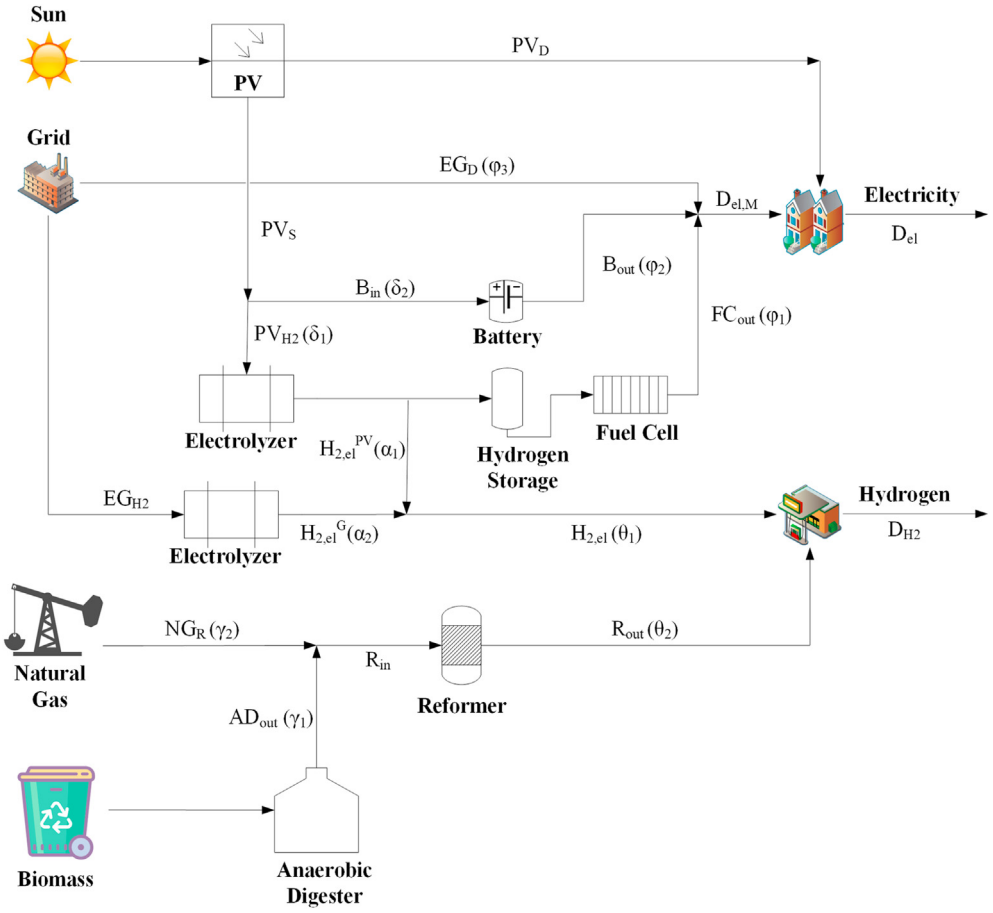

Fig. 2. Energy system flowsheet including energy flows.

$$0 \leq S_B(t) \leq S_{B,max} \quad , \textit{battery storage} \tag{47}$$

$$S_B(t_0) = S_B\left(t_f\right) \quad , \textit{periodicity} \tag{48}$$

$$0 \leq S_{H2}(t) \leq S_{H2,max} \quad , \textit{hydrogen storage} \tag{49}$$

$$S_{H2}(t_0) = S_{H2}\left(t_f\right) \quad , \textit{periodicity} \tag{50}$$

$$\int_{t0}^{tf} AD_{in}dt \leq Bio_D \quad , \textit{biomass available} \tag{51}$$

$$0 \leq u(t) \leq 1 \; ; \; u \ni \{\phi_1, \phi_2, \theta_1, \alpha_1, \delta_1, \gamma_1\} \quad , \textit{optimization variables} \tag{52}$$

$$\sum_{i}^{I} S_i(t) = 1 \quad S \ni \{\phi, \theta, \alpha, \delta, \gamma\} \; , \textit{consistency} \tag{53}$$

Here, J represents each performance criterion, h is a vector that contains the equations of the energy system model, i.e. those presented in Section 2.2. As noted, these expressions are function of the decision variables (u), the state variables (x), the parameters (p), and the time (t). The state variables correspond to those ones that constitute the energy system model but are not used as decision values, e.g. the demands of electricity and hydrogen, the solar irradiance, the energy flows B_{in}, EG_D, $D_{el,M}$ and so on. Besides, $S_B(t)$ and $S_{H2}(t)$ are linked to the imposed path-constraints in order to give physical sense to the level of energy stored (Equations (47) and (49)), and also to end-point constraints for imposing periodic behavior in the storage systems (Equations (48) and (50)), i.e. there is no net accumulation of energy over the evaluated time horizon. Meanwhile, Equation (51) represents a constraint on the amount of biomass available (Bio_D). Besides, u denotes the set of optimization variables, which are linked to the energy flows FC_{out} (ϕ_1), B_{out} (ϕ_2), $H_{2,el}$ (θ_1), $H_{2,el}^{PV}$ (α_1), PV_{H2} (δ_1) and AD_{out} (γ_1).

The optimization problem stated in Equations (43)–(53) was solved taking into account a period of one year, and using a time step of 12 h, i.e. $\Delta t = 12h$, $t_0 = 0h$ and $t_f = 8760h$. This time step allows not only to describe the daily fluctuations of energy demand and availability, but also to decrease the number of optimization variables from 52 860 (1 h time step) to 4380 (12 h time step), which enables to reduce the CPU time for solving the problem. Indeed, the optimizations lasted around 24 h in a computer with an Intel® Xeon® Silver processor and were performed within MATLAB® software using the *fmincon* function and the *SQP* (sequential quadratic programming) algorithm. Some basics about the algorithm could be found in Chapter 18 of Nocedal and Wright [51]. This algorithm was selected because of its speed of convergence. Moreover, *SQP* algorithm can be effectively used if nonlinearities are included in the objective functions and/or the constraints, e.g. by adding part-load efficiencies or economies of scale within the energy system model. Additionally, it is noteworthy that the aim of

this work was focused on the conceptual design stage of the energy system, hence detailed simulations, which could be easily implemented by modifying the time step, are beyond the scope of this study.

2.4. Input data for optimization

Considering the proposed energy system modeling (Section 2.2) and optimization approach (Section 2.3), the required input information for designing the DES is:

a) The time-dependent weather conditions, i.e. ambient temperature and solar irradiance.
b) The time-dependent profiles of electricity and hydrogen demands.
c) The prices of taking energy from the electricity grid and natural gas network.
d) The emission factor of the electricity and natural gas coming from the grid.
e) The technical and cost parameters of each technology. These values refer to the conversion efficiencies, lifetime, investment, and fixed operation and maintenance costs.
f) The energy system constraints, which correspond to the upper limits for the capacity of battery and hydrogen systems. Additionally, the total amount of biomass available is required.

2.4.1. Case study

The case study is a hypothetical community of 1500 inhabitants near Marseille – France. Weather data, namely solar irradiance (Fig. 3a) and ambient temperature (Fig. 3b) were gathered from Solcast webpage [52]. The hourly profile of electricity demand (Fig. 3c) was obtained for 2018 from the Open Data Réseaux Énergies (ODRÉ) [53]. Regarding hydrogen, it is supposed to be used in mobility with a peak demand of 160 kW, which corresponds approximately to a capacity for supplying 60 kg of hydrogen by day (i.e. ≈ 12 cars by day). For this demand, a daily periodic behavior was assumed as presented in Fig. 3d.

The selected prices for importing electricity (C_{EG}) and natural gas (C_{NG}) from the grid are 0.10 €/kWh and 0.037 €/kWh, respectively, which correspond to the values reported by the French energy market in 2018 [54]. Besides, 0.054 €/kg is the cost of gathering the feedstock for anaerobic digestion process (C_{Bio}). Otherwise, the emission factors of electricity (λ_{EG}) and natural gas (λ_{NG}) according to the French energy matrix are 0.057 and 0.040 $kgCO_2/kWh$, respectively [55]. Furthermore, the emission factors of reforming and anaerobic digestion processes are 10 $kgCO_2/kgH_2$ and 0.92 $kgCO_2/m^3CH_4$, respectively. All these values were considered constant along time.

On the other hand, technical and cost parameters for the set of evaluated technologies are presented in Tables S1 and S2 of the supplementary material. These include the energy conversion efficiency, lifetime, and capital, operation, and maintenance costs of each technology.

2.4.2. Energy system constraints

As mentioned in section 2.3.3, the level of energy stored in battery and hydrogen units is constrained by upper limits in their capacities $S_{B,max}$ and $S_{H2,max}$, respectively. Overall, the definition of those limits depends upon the time scale of application (i.e. short-term for battery and long-term for hydrogen), and the generation and consumption profiles of electricity within the energy system. On the one hand, concerning the storage time scale, batteries are identified as a suitable option for storing electricity during days, whereas hydrogen system has the potential for reserving energy by months (seasonal storage) [56–59].

On the other hand, the electricity generated by photovoltaics is a function of the panel efficiency, the solar irradiance, and the installed surface as stated in Equation (1). In this respect, three different values of photovoltaic surface are considered in this work. The minimum area corresponds to that one capable to satisfy the

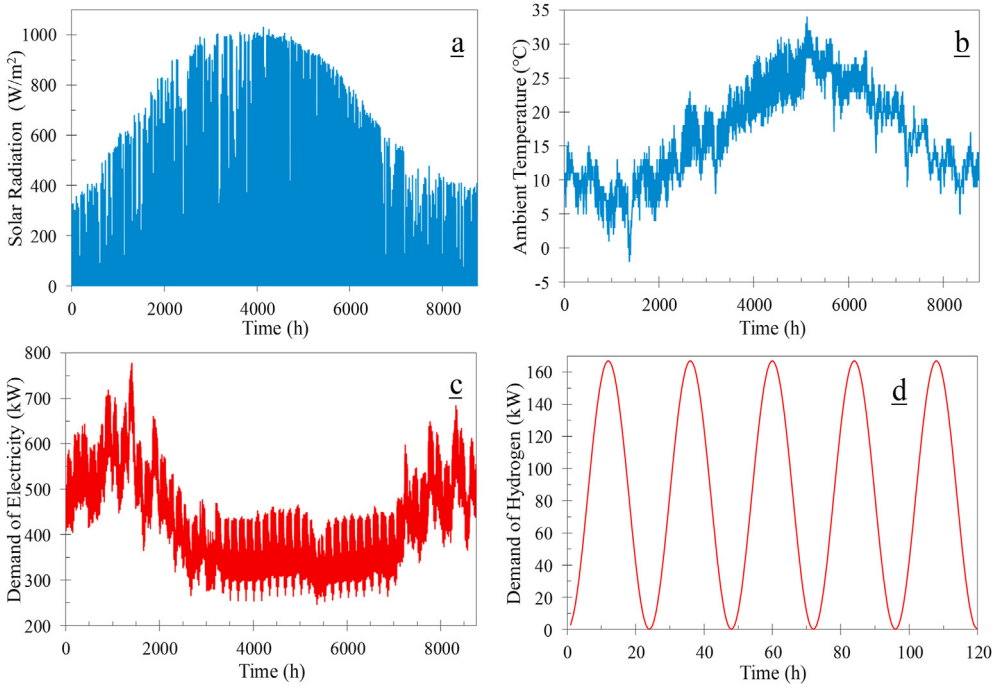

Fig. 3. Profiles of input data for designing the energy system. (a) Solar radiation, (b) ambient temperature, (c) electricity demand, (d) hydrogen demand.

peak electricity demand, which according to Fig. 3c is approximately 800 kW. In such a way, photovoltaic area was computed by dividing the peak demand into the nominal capacity factor of panels, which is around 0.16 kW/m^2 as specified by some manufacturers [60–62]. Therefore, the minimum surface required for satisfying the peak electricity demand is equal to 5000 m^2. The other values evaluated represent scenarios with 50 and 100% of additional area, i.e. 7500 and 10000 m^2.

Taking this into account, the upper limits $S_{B,max}$ and $S_{H2,max}$ were defined for the scenario with the highest electricity production, i.e. with a photovoltaic area of 10 000 m^2. Thus, the maximum capacities of the storage systems were determined considering an isolated system through the pinch analysis and the grand composite curves (GCC) as proposed by Bandyopadhyay [63]. Then, assuming that the battery is able to store energy up to ten days, and the pressurized hydrogen tank up to two months, the upper limits $S_{B,max}$ and $S_{H2,max}$ are 30 MWh and 300 MWh, respectively. The GCC are depicted in Fig. S1 of the supplementary material.

Additionally, the total amount of biomass available (Bio_D) was estimated considering that in France each inhabitant generates 568 kg/year of domestic waste. From such rubbish, around 30% corresponds to organic matter that can be used in the digestion process, so that the biomass available is 255.6 ton/year [64,65].

3. Results and discussion

The optimization of the energy system design was solved for the three surfaces of photovoltaic panels, and considering each criterion individually, i.e. three optimization problems were solved for minimizing the total annualized cost, the CO_2 emissions, and the grid dependence. Fig. 4 depicts the resulting energy system configuration for each objective optimized separately, and for installed photovoltaic areas of 5000, 7500 and 10 000 m^2.

In general, through the obtained configurations, results show the influence of the evaluated criteria on the selection of technologies for satisfying the energy needs. Additionally, the installed surface of photovoltaic panels also affects the energy system flowsheet. Indeed, for the three evaluated objective functions, the optimal set of technologies with 5000 m^2 of photovoltaic panels differs from the ones obtained when the area is 7500 or 10 000 m^2.

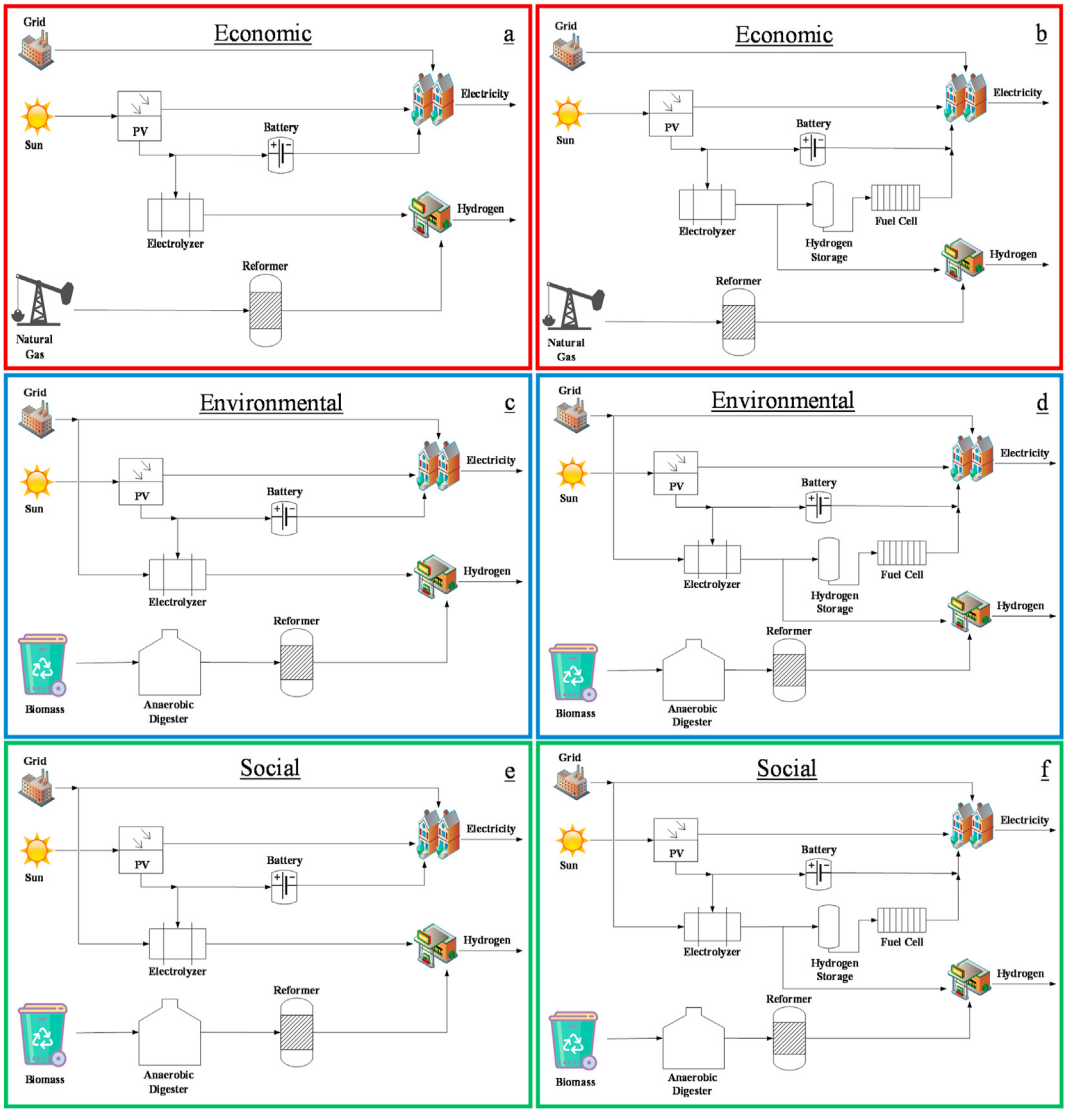

Fig. 4. Optimal configuration of the distributed energy system. (left column) 5000 m^2, (right column) 7500–10000 m^2. Optimization objective (a, b) economic, (c, d) environmental, (e, f) social.

This is observed by comparing Fig. 4a and b for economic objective, Fig. 4c and d for environmental criterion, and Fig. 4e and f for social objective. In those cases, the most significant difference concerns to the storage unit. In fact, in the case wherein the smallest size of panels is considered (5000 m^2), there is no need of storing a large amount of electricity during long periods, and hence just the battery is employed (Fig. 4a–c and 4e).

Interestingly, the optimal energy system flowsheet is the same from the environmental and social perspective (Fig. 4c and e for 5000 m^2, and Fig. 4d and f for 7500 and 10 000 m^2). In this regard, it is worth noting that this result strongly relies upon the considered context and some technical parameters (e.g. conversion efficiency). On the one hand, as the case study of this work is in France, and negligible deforestation was assumed, biomass represents the best alternative when the objective is to minimize either the CO_2 emissions or the grid dependence. However, in a context with significative deforestation rate, or an energy matrix based on fossil resources, the optimization of environmental and social objectives could lead to different system structures. Indeed, this issue was verified by carrying out a sensitivity analysis with those two parameters. Thus, the environmental optimization was solved for three different values of deforestation rate (ω) 10, 20 and 30%, and the impact of this parameter on the energy system structure was evidenced. The corresponding results are depicted in Table S3 and Fig. S2 of the supplementary material.

On the other hand, the impact of the electricity grid emission factor was evaluated by assuming the one of Germany, which was roughly 0.48 $kgCO_2/kWh$ in 2018 [66]. In this case, environmental and social optimizations were performed for determining the influence of this value on the system flowsheet. Results are presented in Table S4 and Fig. S3 of the supplementary material. According to these optimization results, it is observed that the conversion efficiency is the key parameter for selecting the electricity grid instead of methane for obtaining hydrogen when the objective is to decrease the energy imported from the grid (Fig. 4e and f). This happens because for producing 1 kg of hydrogen, the energy consumption of the electrolyzer and methane reforming units are 51.3 and 65.4 kWh, respectively (Table S1). Meanwhile, from the environmental perspective the choice of the energy source lies on the emission factor of the alternatives. Therefore, when the French grid is employed, water electrolysis ($\approx$3 $kgCO_2/kgH_2$) is preferred instead of methane reforming ($\approx$12 $kgCO_2/kgH_2$), as presented in Fig. 4c and d. Conversely, if the electricity grid of Germany is used ($\approx$24 $kgCO_2/kgH_2$), steam methane reforming would be privileged (Fig. S3a).

Otherwise, if the photovoltaic area is 7500 or 10 000 m^2, there is no effect of this variable upon the selected technologies and the flowsheet structure, but the operating policy changes. Hence, the energy system design exclusively relies on the objective function as observed by comparing Fig. 4b, d and 4f. Thus, when only the economic index is considered (Fig. 4b), hydrogen is mainly produced via methane reforming ($\approx$48–60%) due to the lower cost of natural gas with respect to the electricity. In fact, in this case the electrolyzer is just powered by photovoltaic panels and biomass is not included within the system. Meanwhile, if environmental or social objectives are addressed (Fig. 4d and e), around 83% of hydrogen is obtained from water electrolysis, and the remainder is covered by reforming of biomethane derived from biomass digestion. This happens because, when the electrolyzer is used, environmental impact only depends on the emission factor of the electricity grid, which in the case of France is relatively low due to the massive electricity production from nuclear plants. Additionally, in these cases the whole biomass available is employed because it does not imply any CO_2 emission and is not grid reliant.

Main optimization results for the three evaluated photovoltaics surfaces are summarized in Table 1. These results show the conflicting character of the objectives and the contribution of the different factors (CAPEX, OPEX, grid, process, electricity, and natural gas) to each performance criterion. Minimal costs are associated with mature technologies (steam methane reforming) and fossil resources, which leads to the highest CO_2 emissions and grid dependence. In contrast, large use of biomass and emission-free operations (electrolysis) would increase the self-sufficiency of the system but at the cost of higher investment. Besides, as observed in Table 1, when environmental and social criteria are optimized, all the emissions come from the electricity grid. Indeed, in these cases an important amount of CO_2 is derived from biomass transformation and, as aforementioned, these emissions are not accounted because they are supposed to be compensated during the growing up of plants. On the other hand, the investment cost of each technology for the three objective functions and the different photovoltaic surfaces is presented in Table 2.

As previously mentioned, when a photovoltaic area of 5000 m^2 is considered, the optimal configuration of the system indicates that just the battery is required for energy storage. In fact, as verified in Fig. 5a, the battery mainly operates in spring and summer seasons, and the optimization objective does not have a notable impact on its size and operating policy. On the contrary, when photovoltaic area of 7500 and 10 000 m^2 are evaluated, electricity production increases and, consequently, short and long-term storage systems are used in all the optimization cases (Fig. 6).

Broadly, it is observed that the battery is mainly used as a short-term storage system, i.e. for storing energy during days or weeks (Fig. 6a and c). Meanwhile, hydrogen absorbs the mismatch between electricity availability and consumption in the middle and long-term, and therefore it exhibits a seasonal pattern, as depicted in Fig. 6b and d. In those cases, pressurized tank starts to be charged at spring ($t \approx 2500$ h), and a significant change in the slope of the

Table 1
Optimization results for the design of the distributed energy system.

Variable	PV area = 5000 m^2			PV area = 7500 m^2			PV area = 10 000 m^2		
	Eco.	Envi.	Social	Eco.	Envi.	Social	Eco.	Envi.	Social
TAC (M€/year)	0.9	1.5	1.5	1.8	2.5	2.5	2.4	2.8	2.8
CAPEX (% TAC)	73	74	74	90	91	91	93	94	94
OPEX (% TAC)	27	26	26	10	9	9	7	6	6
CO_2 emissions (ton/year)	345.1	145.6	145.6	227.7	81.7	81.7	176.0	51.2	51.2
Grid emissions (%)	43	100	100	37	100	100	34	100	100
Process emissions (%)	57	–	–	63	–	–	66	–	–
Biogenic (ton/year)	–	62.9	62.9	–	62.9	62.9	–	62.9	62.9
Dependence (%)	63	52	52	40	30	30	30	19	19
Electricity (%)	57	100	100	56	100	100	53	100	100
Natural gas (%)	43	–	–	44	–	–	47	–	–

Table 2
Optimal investment cost (k€/year) of the equipment within the energy system.

Equipment	PV area = 5000 m^2		PV area = 7500 m^2		PV area = 10 000 m^2	
	Eco.	Envi. - Social	Eco.	Envi. - Social	Eco.	Envi. - Social
Photovoltaics	103.8		155.8		207.7	
Electrolyzer	68.9	68.8	211.2	205.3	413.6	377.6
Battery	406.5	801.4	965.6	1712.8	1249.5	1712.8
Reformer	55.0	54.7	55.0	44.2	55.0	44.2
Hydrogen Storage	–	–	85.2	119.7	101.9	203.9
Fuel Cell	–	–	122.1	48.9	174.4	90.7
Digester	–	49.2	–	39.0	–	39.0

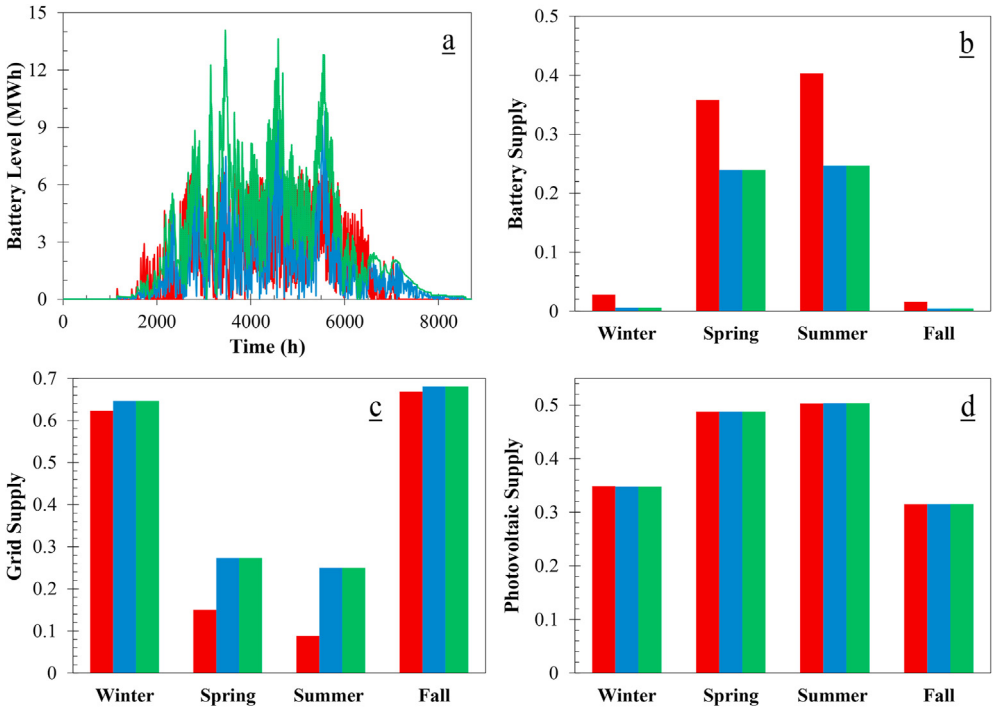

Fig. 5. Optimal profile of energy stored (a), and fractions of electricity supplied by the battery (b), the grid (c), and the photovoltaic panels (d) considering 5000 m^2 of photovoltaic surface. Objective (—) economic, (—) environmental, (—) social.

curve is observed at the beginning of summer season ($t \approx 4000$ h). Then, during fall and winter seasons the tank is discharged for covering the lack of electricity from photovoltaics ($t < 2000$ h and 7500 h $< t <$ 8760 h).

On the other hand, as a result of the high availability of electricity during summer season, if the photovoltaic surface is 10 000 m^2 and environmental or social objectives are addressed, the amount of energy stored reaches up to the limits imposed in the optimization problem, i.e. 30 and 300 MWh for the Li-ion battery and the pressurized hydrogen tank, respectively. In this respect, a sensitivity analysis on the values of the storage limits was performed aiming to evaluate their impact on the optimization results. Thus, the optimization problem was solved by modifying the storage capacities ±10%, i.e. 27 and 33 MWh for the battery, and 270 and 330 MWh for the pressurized tank. The analysis was carried out for the environmental criterion, and according to the results, changes lower than 2% on the objective function are obtained (Table 3).

As observed in Fig. 6, economic optimization leads to smaller storage units, since these represent roughly 60–65% of the CAPEX. Conversely, environmental and social objectives require bigger capacities for energy storage. This occurs because the energy stored corresponds to renewable one, thus, as the capacity for storing this energy increases, less energy must be imported from the grid and, therefore, lower emissions and grid dependence are obtained. In this regard, even though the overall results of environmental and social optimization are the same, the operating policy of the storage systems is quite similar, but it does not overlap. This happens because the system can reach an identical global performance through different operating patterns, which was verified by solving the optimization problem with different initial values of the decision variables. The corresponding results are presented in Fig. S4 of the supplementary material.

Moreover, Fig. 5b–d (5000 m^2 of photovoltaics), and Fig. 7 (7500 and 10 000 m^2 of photovoltaics) present the average fraction of electricity supplied by the battery, the fuel cell, the main electricity grid and the photovoltaic panels for the different seasons of the year. These results indicate a direct relation between the installed surface of photovoltaic panels and the use of the power-to-power system (electrolyzer – hydrogen tank – fuel cell). This fact is observed by comparing the fraction of electricity supplied by the battery (Fig. 7a and b), and the fuel cell (Fig. 7c and d). Here is noted that, as the photovoltaic surface gets larger, the use of long-term storage increases to balance the system during sunny periods

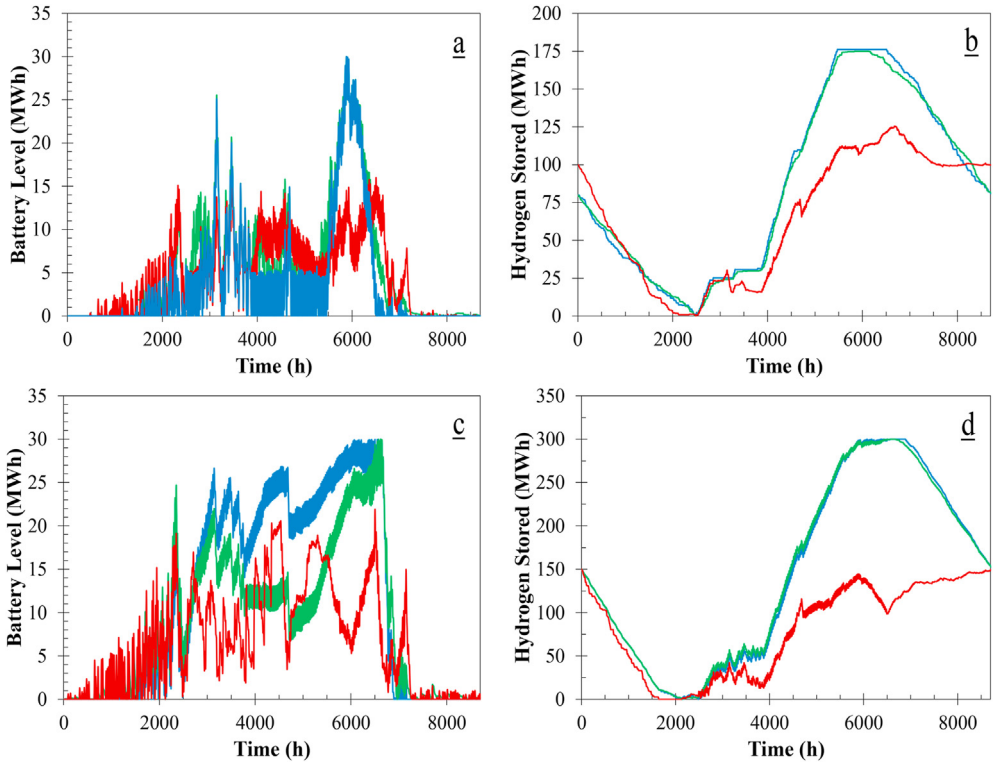

Fig. 6. Optimal profiles of energy stored in battery and pressurized tank. (a, b) 7500 m^2, (c, d) 10 000 m^2. Objective (—) economic, (—) environmental, (—) social.

Table 3
Results of the sensitivity analysis with respect to the storage capacities.

Storage option	Max. capacity (MWh)	CO_2 emissions (ton/year)	Relative difference[a] (%)
Pressurized tank	330	50.2	−1.9
	270	52.1	1.9
Battery	33	51	−0.4
	27	51.3	0.4

[a] The reference case corresponds to 51.2 tonCO_2/year.

(spring and summer). Additionally, as shown in Fig. 7f, the system becomes completely autonomous during spring and summer seasons for all the assessed objectives, which implies that the whole electricity demand can be supplied by renewable resources and without generating CO_2 emissions. This self-sufficiency is achieved thanks to the storage systems, which enable either satisfying the energy demands at nighttime periods or storing the overproduction of electricity to be used during cold seasons. Indeed, this seasonal storage permits to meet up to 76% of the electricity needs at winter, and up to 62% at fall with energy coming from renewables. The fraction supplied by photovoltaics (Figs. 5d, 7g and 7h) corresponds to the electricity delivered to users at the time that it is obtained, i.e. without passing through storage systems.

Aiming to show the potential impact of distributed energy system implementation, a conventional system or centralized case was evaluated for comparison purposes. This centralized case corresponds to the scenario wherein the whole electricity demand is satisfied by energy coming from the main grid, and the hydrogen demand is supplied by a large-scale methane reforming process through the gas network.

Fig. 8 depicts comparatively the performance of the distributed and centralized energy system by considering the optimization results presented in Table 1. This figure represents normalized values, being 1 the best value (minimum), and 0 the worst one (maximum) of the index. Thus, the farther the vertex of the triangle is from the center, the better is its performance in the corresponding criterion. For instance, taking the centralized case as reference, it looks like a line because this case offers the best economic but the worst social and environmental performance. This happens due to the economy of scale and the maturity of the process carried out in centralized energy conversion, which leads to lower levelized cost (€/kWh) for obtaining electricity and hydrogen. However, this scenario also entails the high CO_2 emissions derived from the methane steam reforming process, and a complete dependence on the main energy network.

Moreover, it is noted the potential improvement that can be obtained in the environmental and social criteria with the implementation of the DES, and the effect of the area of photovoltaic panels. For instance, when an area of 5000 m^2 is considered, over cost of 13% is needed in the economic optimization, but at the same time, autonomy reach a value near to 40%, and 25% of CO_2 emissions could be avoided with respect to centralized scenario. Conversely, by using 10 000 m^2 of surface, CO_2 emission reduction up to 89%, and self-sufficiency up to 81% can be achieved, but the cost is more than three times bigger than the one of importing energy from the grid (environmental and social optimizations).

Thus, according to these optimization results and the competitiveness of the criteria, the selection of the most suitable system

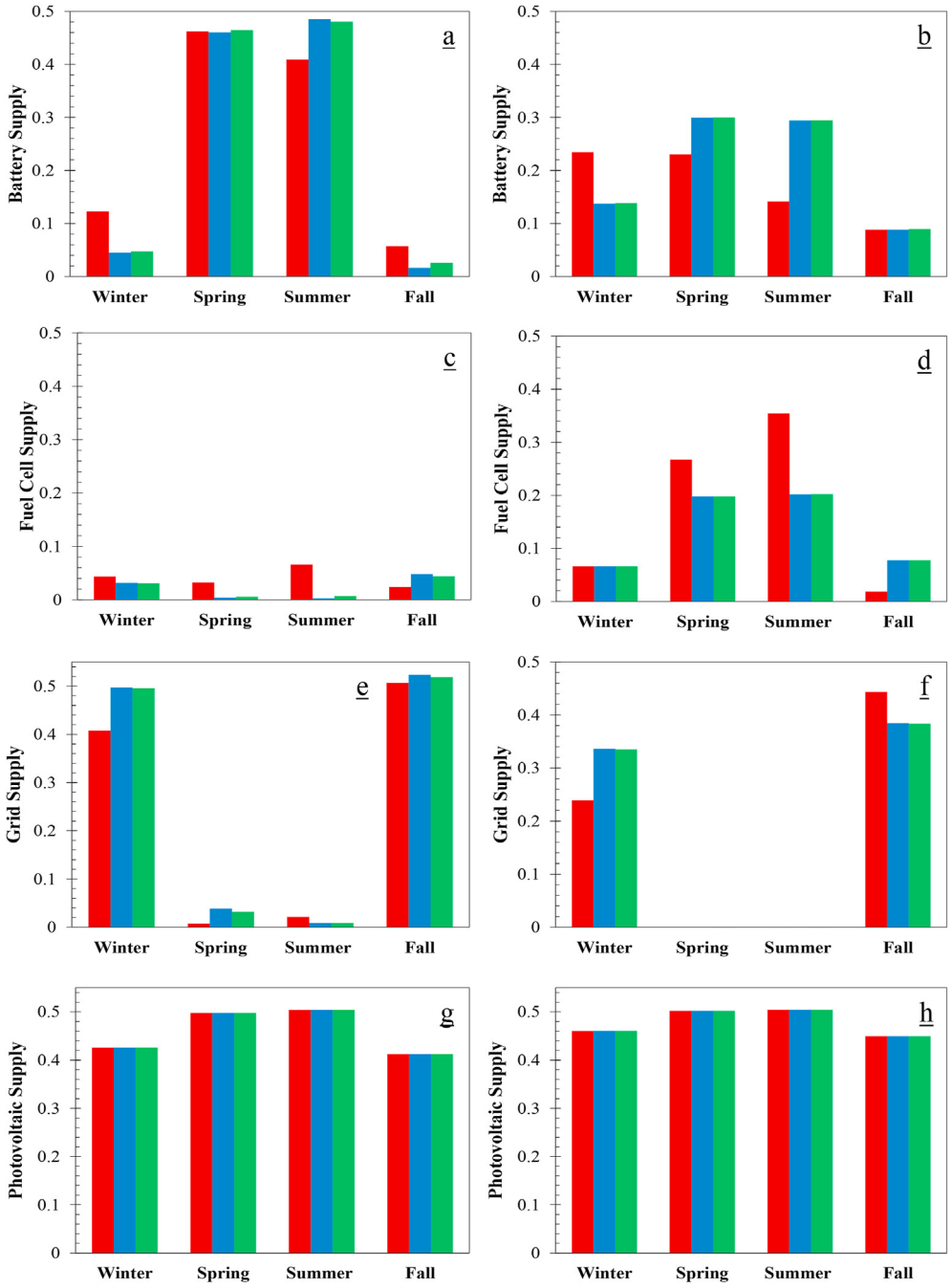

Fig. 7. Optimal fraction of electricity supplied by the distributed energy system considering two surfaces of photovoltaic panels. 7500 m^2 - left column, 10 000 m^2 – right column. Sources: battery (a, b), fuel cell (c, d), main grid (e, f) and photovoltaic panel (g, h). Objective functions: (■) economic, (■) environmental, (■) social.

configuration will depend upon the context wherein the energy system would be implemented, and the preferences/needs of decision-makers. In such a way, the approach presented in this work could be easily extended and applied according to another conditions (e.g. energy sources, energy demands, weather conditions, available technologies), and constitute a tool for evaluating scenarios and support the decision-making process during the design of DES.

4. Conclusions

In this work, a modeling and optimization approach for designing distributed energy systems (DES) was developed. The proposed model considered a grid-connected energy system, and a set of technologies for energy conversion that allows to satisfy electricity and hydrogen needs. The optimization problem consisted in the evaluation of economic, environmental and social criteria, considering as objective functions the total annualized cost, the CO_2 emissions, and the grid dependence, respectively. Results allowed to identify a significant influence of the criteria and the photovoltaic surface upon the energy system structure and its time-dependent operating policy. In this regard, the obtained results represent a quantitative evaluation of different scenarios, and it was found a notable improvement of DES with respect to a

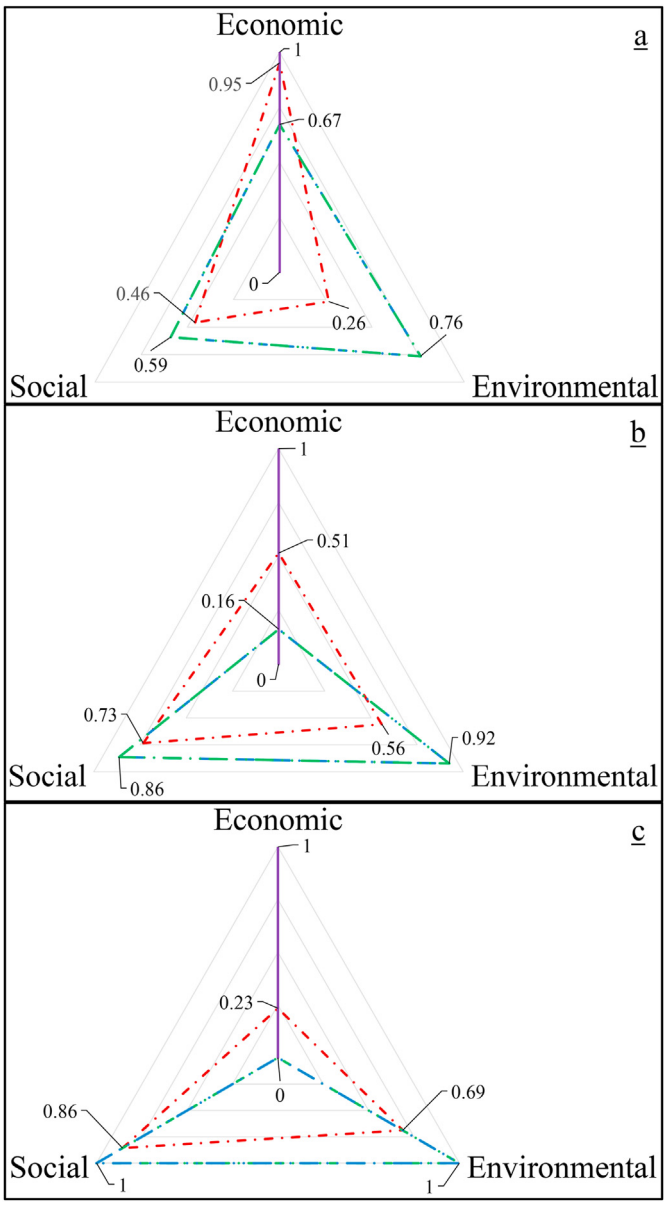

Fig. 8. Representation of the optimization results for the three surfaces of photovoltaic panels. (a) 5000 m^2, (b) 7500 m^2, (c) 10 000 m^2. Objective (— •) economic, (— •) environmental, (— •) social. (—) centralized scenario. Normalized values are presented, being 1 (vertex -outer triangle) the best value, and 0 (center) the worst value of the index.

centralized energy system in terms of emissions and self-sufficiency. Thus, the emission up to 400 tonCO_2/year could be avoided (with respect to the centralized scenario), and the main grid dependency could be reduced to below 20%. Indeed, even with the smallest photovoltaic area (5000 m^2) and without seasonal energy storage, 25% of the CO_2 emissions could be prevented and near to 40% of self-sufficiency could be achieved. Furthermore, this approach can be easily extended by including additional energy sources or demands, conversion technologies and performance criteria to be applied in another context conditions. As a perspective, it is envisaged to use the proposed approach within a multi-objective optimization analysis. This could enable to establish the relationships among the sustainability criteria, and to integrate the preferences of decision-makers at conceptual design of DES.

Credit author statement

Juan D. Fonseca — Conceptualization, Methodology, Software, Investigation, Writing - original draft. Jean-Marc Commenge — Conceptualization, Software, Writing - review & editing, Supervision. Mauricio Camargo — Conceptualization, Writing - review & editing, Supervision, Resources, Funding acquisition. Laurent Falk — Conceptualization, Writing - review & editing, Supervision, Resources, Funding acquisition. Iván D. Gil — Conceptualization, Writing - review & editing, Supervision

Declaration of competing interest

The authors declare that they have no known competing financial interests or personal relationships that could have appeared to influence the work reported in this paper.

Acknowledgment

This work was supported partly by the french PIA project « Lorraine Université d'Excellence », reference ANR-15-IDEX-04-LUE »

Appendix A. Supplementary data

Supplementary data to this article can be found online at https://doi.org/10.1016/j.energy.2020.118989.

References

[1] Alanne K, Saari A. Distributed energy generation and sustainable development. Renew Sustain Energy Rev 2006;10:539–58. https://doi.org/10.1016/j.rser.2004.11.004.
[2] Fonseca JD, Camargo M, Commenge JM, Falk L, Gil ID. Trends in design of distributed energy systems using hydrogen as energy vector: a systematic literature review. Int J Hydrogen Energy 2019;44:9486–504. https://doi.org/10.1016/j.ijhydene.2018.09.177.
[3] Bouffard F, Kirschen DS. Centralised and distributed electricity systems. Energy Pol 2008;36:4504–8. https://doi.org/10.1016/j.enpol.2008.09.060.
[4] Shivarama Krishna K, Sathish Kumar K. A review on hybrid renewable energy systems. Renew Sustain Energy Rev 2015;52:907–16. https://doi.org/10.1016/j.rser.2015.07.187.
[5] Mazloomi K, Gomes C. Hydrogen as an energy carrier: prospects and challenges. Renew Sustain Energy Rev 2012;16:3024–33. https://doi.org/10.1016/j.rser.2012.02.028.
[6] International Energy Agency (IEA). The future of hydrogen. 2019.
[7] Parra D, Valverde L, Pino FJ, Patel MK. A review on the role, cost and value of hydrogen energy systems for deep decarbonisation. Renew Sustain Energy Rev 2019;101:279–94. https://doi.org/10.1016/j.rser.2018.11.010.
[8] Nastasi B, Lo Basso G. Hydrogen to link heat and electricity in the transition towards future Smart Energy Systems. Energy 2016;110:5–22. https://doi.org/10.1016/j.energy.2016.03.097.
[9] Dincer I, Acar C. Smart energy solutions with hydrogen options. Int J Hydrogen Energy 2018;43:8579–99. https://doi.org/10.1016/j.ijhydene.2018.03.120.
[10] Liu P, Georgiadis MC, Pistikopoulos EN. An energy systems engineering approach for the design and operation of microgrids in residential applications. Chem Eng Res Des 2013;91:2054–69. https://doi.org/10.1016/j.cherd.2013.08.016.
[11] Mavromatidis G, Orehounig K, Bollinger LA, Hohmann M, Marquant JF, Miglani S, et al. Ten questions concerning modeling of distributed multi-energy systems. Build Environ 2019;165:106372. https://doi.org/10.1016/j.buildenv.2019.106372.
[12] Adil AM, Ko Y. Socio-technical evolution of Decentralized Energy Systems: a critical review and implications for urban planning and policy. Renew Sustain Energy Rev 2016;57:1025–37. https://doi.org/10.1016/j.rser.2015.12.079.
[13] International Renewable Energy Agency (IRENA). Global Energy transformation:A roadmap to 2050. 2018.
[14] Mehleri ED, Sarimveis H, Markatos NC, Papageorgiou LG. A mathematical programming approach for optimal design of distributed energy systems at the neighbourhood level. Energy 2012;44:96–104. https://doi.org/10.1016/j.energy.2012.02.009.
[15] Yang Y, Zhang S, Xiao Y. An MILP (mixed integer linear programming) model for optimal design of district-scale distributed energy resource systems. Energy 2015;90:1901. https://doi.org/10.1016/j.energy.2015.07.013.
[16] Schütz T, Hu X, Fuchs M, Müller D. Optimal design of decentralized energy

conversion systems for smart microgrids using decomposition methods. Energy 2018;156:250–63. https://doi.org/10.1016/j.energy.2018.05.050.
[17] Pan G, Gu W, Wu Z, Lu Y, Lu S. Optimal design and operation of multi-energy system with load aggregator considering nodal energy prices. Appl Energy 2019;239:280–95. https://doi.org/10.1016/j.apenergy.2019.01.217.
[18] Dorotić H, Pukšec T, Duić N. Economical, environmental and exergetic multi-objective optimization of district heating systems on hourly level for a whole year. Appl Energy 2019;251:113394. https://doi.org/10.1016/j.apenergy.2019.113394.
[19] Dorotić H, Pukšec T, Duić N. Multi-objective optimization of district heating and cooling systems for a one-year time horizon. Energy 2019;169:319–28. https://doi.org/10.1016/j.energy.2018.11.149.
[20] Maroufmashat A, Sattari S, Roshandel R, Fowler M, Elkamel A. Multi-objective optimization for design and operation of distributed energy systems through the multi-energy hub network approach. Ind Eng Chem Res 2016;55:8950–66. https://doi.org/10.1021/acs.iecr.6b01264.
[21] Falke T, Krengel S, Meinerzhagen AK, Schnettler A. Multi-objective optimization and simulation model for the design of distributed energy systems. Appl Energy 2016;184:1508–16. https://doi.org/10.1016/j.apenergy.2016.03.044.
[22] Gabrielli P, Gazzani M, Martelli E, Mazzotti M. Optimal design of multi-energy systems with seasonal storage. Appl Energy 2018;219:408–24. https://doi.org/10.1016/j.apenergy.2017.07.142.
[23] Fazlollahi S, Becker G, Ashouri A, Maréchal F. Multi-objective, multi-period optimization of district energy systems: IV - a case study. Energy 2015;84:365–81. https://doi.org/10.1016/j.energy.2015.03.003.
[24] Rieder A, Christidis A, Tsatsaronis G. Multi criteria dynamic design optimization of a small scale distributed energy system. Energy 2014;74:230–9. https://doi.org/10.1016/j.energy.2014.06.007.
[25] Pelet X, Favrat D, Leyland G. Multiobjective optimisation of integrated energy systems for remote communities considering economics and CO2 emissions. Int J Therm Sci 2005;44:1180–9. https://doi.org/10.1016/j.ijthermalsci.2005.09.006.
[26] Li L, Mu H, Li N, Li M. Economic and environmental optimization for distributed energy resource systems coupled with district energy networks. Energy 2016;109:947–60. https://doi.org/10.1016/j.energy.2016.05.026.
[27] Di Somma M, Yan B, Bianco N, Graditi G, Luh PB, Mongibello L, et al. Design optimization of a distributed energy system through cost and exergy assessments. Energy Procedia 2017;105:2451–9. https://doi.org/10.1016/j.egypro.2017.03.706.
[28] Fazlollahi S, Mandel P, Becker G, Maréchal F. Methods for multi-objective investment and operating optimization of complex energy systems. Energy 2012;45:12–22. https://doi.org/10.1016/j.energy.2012.02.046.
[29] Ren H, Zhou W, Nakagami K, Gao W, Wu Q. Multi-objective optimization for the operation of distributed energy systems considering economic and environmental aspects. Appl Energy 2010;87:3642–51. https://doi.org/10.1016/j.apenergy.2010.06.013.
[30] Di Somma M, Yan B, Bianco N, Luh PB, Graditi G, Mongibello L, et al. Multi-objective operation optimization of a Distributed Energy System for a large-scale utility customer. Appl Therm Eng 2016;101:752–61. https://doi.org/10.1016/j.applthermaleng.2016.02.027.
[31] Di Somma M, Graditi G, Heydarian-Forushani E, Shafie-khah M, Siano P. Stochastic optimal scheduling of distributed energy resources with renewables considering economic and environmental aspects. Renew Energy 2018;116:272–87. https://doi.org/10.1016/j.renene.2017.09.074.
[32] Dufo-López R, Bernal-Agustín JL. Multi-objective design of PV-wind-diesel-hydrogen-battery systems. Renew Energy 2008;33:2559–72. https://doi.org/10.1016/j.renene.2008.02.027.
[33] Eriksson ELV, Gray EMA. Optimization of renewable hybrid energy systems – a multi-objective approach. Renew Energy 2019;133:971–99. https://doi.org/10.1016/j.renene.2018.10.053.
[34] Floudas CA. Nonlinear and mixed-integer optimization: fundamentals and applications. Oxford University Press; 1995.
[35] Edgar TF, Himmelblau DM. Optimization of chemical process. Second. New York: McGRAW-HILL; 2001.
[36] Frangopoulos CA. Recent developments and trends in optimization of energy systems. Energy 2018;164:1011–20. https://doi.org/10.1016/j.energy.2018.08.218.
[37] International atomic energy agency (IAEA), united nations department of economic and social affairs, international energy agency (IEA), EUROSTAT, European environment agency. Energy Indicators for Sustainable Development : Guidelines and; 2005.
[38] García-Serna J, Pérez-Barrigón L, Cocero MJ. New trends for design towards sustainability in chemical engineering: green engineering. Chem Eng J 2007;133:7–30. https://doi.org/10.1016/j.cej.2007.02.028.
[39] United Nations. Sustainable development goals. Goal 7 afford clean energy n.d. https://www.un.org/sustainabledevelopment/energy/. [Accessed 12 May 2020].
[40] Mikhail J, Gallego-schmid A, Stamford L, Azapagic A. Design and environmental sustainability assessment of small-scale off-grid energy systems for remote rural communities. Appl Energy 2020;258:114004. https://doi.org/10.1016/j.apenergy.2019.114004.
[41] Santoyo-Castelazo E, Azapagic A. Sustainability assessment of energy systems: integrating environmental, economic and social aspects. J Clean Prod 2014;80:119–38. https://doi.org/10.1016/j.jclepro.2014.05.061.
[42] Koirala BP, Koliou E, Friege J, Hakvoort RA, Herder PM. Energetic communities for community energy: a review of key issues and trends shaping integrated community energy systems. Renew Sustain Energy Rev 2016;56:722–44. https://doi.org/10.1016/j.rser.2015.11.080.
[43] Gallego Carrera D, Mack A. Sustainability assessment of energy technologies via social indicators: results of a survey among European energy experts. Energy Pol 2010;38:1030–9. https://doi.org/10.1016/j.enpol.2009.10.055.
[44] Ribeiro F, Ferreira P, Araújo M. The inclusion of social aspects in power planning. Renew Sustain Energy Rev 2011;15:4361–9. https://doi.org/10.1016/j.rser.2011.07.114.
[45] Rösch C, Bräutigam K, Kopfmüller J, Stelzer V, Lichtner P. Indicator system for the sustainability assessment of the German energy system and its transition. Energy Sustain Soc 2017;7:1–13. https://doi.org/10.1186/s13705-016-0103-y.
[46] Stamford L, Azapagic A. Sustainability indicators for the assessment of nuclear power. Energy 2011;36:6037–57. https://doi.org/10.1016/j.energy.2011.08.011.
[47] Skoplaki E, Palyvos JA. On the temperature dependence of photovoltaic module electrical performance: a review of efficiency/power correlations. Sol Energy 2009;83:614–24. https://doi.org/10.1016/j.solener.2008.10.008.
[48] Thrän D, Billig E, Persson T, Svensson M, Daniel-Gromke J, Ponitka J, et al. Biomethane status and factors affecting market development and trade. 2014.
[49] Pramanik SK, Suja FB, Zain SM, Pramanik BK. The anaerobic digestion process of biogas production from food waste: prospects and constraints. Bioresour Technol Reports 2019;8:100310. https://doi.org/10.1016/j.biteb.2019.100310.
[50] (ADEME). Agence de l'Environnement et de la Maîtrise de l'Energie. CO2 Biogénique. Bilans GES; 2019. http://www.bilans-ges.ademe.fr/documentation/UPLOAD_DOC_FR/index.htm?co2_biogenique.htm. [Accessed 11 December 2019].
[51] Nocedal J, Wright SJ. Numerical optimization. second ed., vol. 17. New York: Springer; 2006. https://doi.org/10.1097/00003446-199604000-00005.
[52] Solcast. Solar forecasting & solar irradiance data. 2019. https://solcast.com/. [Accessed 16 June 2019].
[53] Open Data Réseaux Énergies (ODRÉ). Consommation quotidienne brute. 2012.
[54] Ministère de la Transition Écologique et Solidaire. Données et études statistiques Pour le changement climatique, l'énergie, l'environnement, le logement, et les transports. 2019. https://www.statistiques.developpement-durable.gouv.fr/prix-de-lenergie-0?rubrique=22. [Accessed 3 April 2019].
[55] (ADEME) Agence de l'Environnement et de la Maîtrise de l'Energie. Données - base Carbone. Bilans GES; 2019. http://www.bilans-ges.ademe.fr/. [Accessed 15 December 2019].
[56] Chen H, Ngoc T, Yang W, Tan C, Li Y. Progress in electrical energy storage system : a critical review. Prog Nat Sci 2009;19:291–312. https://doi.org/10.1016/j.pnsc.2008.07.014.
[57] Ajanovic A, Hiesl A, Haas R. On the role of storage for electricity in smart energy systems. Energy 2020;200:117473. https://doi.org/10.1016/j.energy.2020.117473.
[58] Luo X, Wang J, Dooner M, Clarke J. Overview of current development in electrical energy storage technologies and the application potential in power system operation. Appl Energy 2015;137:511–36. https://doi.org/10.1016/j.apenergy.2014.09.081.
[59] Aneke M, Wang M. Energy storage technologies and real life applications – a state of the art review. Appl Energy 2016;179:350–77. https://doi.org/10.1016/j.apenergy.2016.06.097.
[60] WINAICO. Photovoltaic modules. Prod datasheets. http://www.winaico.com/photovoltaik/modules/wsp-m6-perc-mono/. [Accessed 4 September 2019].
[61] LG electronics inc. Solar - products. Sol bus div. https://www.lg.com/global/business/solar. [Accessed 4 September 2019].
[62] Mitsubishi electric. Solar solutions. Specif sheets. https://www.mitsubishielectricsolar.com/products/residential/solar_modules. [Accessed 4 September 2019].
[63] Bandyopadhyay S. Design and optimization of isolated energy systems through pinch analysis. Asia Pac J Chem Eng 2011;518–26. https://doi.org/10.1002/apj.
[64] (ADEME) Agence de l'Environnement et de la Maîtrise de l'Energie. MODECOM 2017 Campagne nationale de caractérisation des déchets ménagers et assimilés. Angers; 2019.
[65] (ADEME) Agence de l'Environnement et de la Maîtrise de l'Energie. Déchets chiffres-clés. Angers; 2018.
[66] Agora energiewende. Recent electricity data. Power price emiss. https://www.agora-energiewende.de/en/service/recent-electricity-data/chart/power_price_emission/01.01.2018/31.12.2018/. [Accessed 8 June 2020].